# Removal of RFI in Wideband Radars

Charles TC Le, Scott Hensley, and Elaine Chapin
Jet Propulsion Laboratory. MS: 300-235.
4800 Oak Grove Drive, Pasadena, CA 91109.
Phone: (818)354-4633. Fax: (818)393-5285. Email: cle@radar-sci.jpl.nasa.gov

**Abstract** The least-mean-square (LMS) adaptive filter is applied to suppress narrow-band radio-frequency interference (RFI) in wideband synthetic aperture radar (SAR) signals. Simulation is used to show the working principles of the adaptive filter and to obtain the optimum filter's parameters. The algorithm is tested with P-band synthetic aperture radar (SAR) data collected by the NASA/JPL airborne SAR (AIRSAR) in different noisy environments.

## INTRODUCTION

The dual requirement of a low radar frequency for foliage and/or ground penetration and a wide radar bandwidth for high resolution in wideband radar systems leads to radars operating in frequency bands occupied by other radio systems, such as radio communications, navigation, police, emergency rescue, ... [1, 2]. In this study, we will apply the LMS algorithm [3, 4] to remove narrow-band RFI from wideband SAR signals. We first formulate the LMS algorithm and describe the point target simulator. We then show the output of the pulse compression filter. Finally, we show cleaned images obtained by applying the adaptive filter to data collected by the NASA/JPL P-band TOPSAR/AIRSAR system [5] and processed with an interferometric SAR processor developed at JPL [6].

## THE LMS ALGORITHM

The LMS adaptive filter is shown in Fig. 1. For each iteration when the next sample is available, the weights of the transversal filter are adapted according to the following equations

$$\mathbf{w}(n+1) = \mathbf{w}(n) + \mu \mathbf{x}(n) e^*(n) \qquad (1)$$

where

$$\begin{aligned}
\mathbf{w}(n) &= \text{complex filter weights on the } n^{th} \text{ iteration} \\
&= [w_0(n), w_1(n), \ldots, w_{L-1}(n)]^T \\
e(n) &= \text{error signal} = d(n) - y(n) \\
y(n) &= \text{filter output} = \mathbf{w}^T(n) \cdot \mathbf{x}(n) \\
d(n) &= \text{input signal} \\
x(n) &= \text{reference signal} = d(n - \Delta) \\
\mathbf{x}(n) &= \text{L-dimension reference vector} \\
&= [x(n), x(n-1), \ldots, x(n-L+1)]^T \\
\mu &= \text{constant step-size parameter} \\
\Delta &= \text{constant decorrelation parameter} \\
L &= \text{filter length}
\end{aligned}$$

## THE POINT-TARGET SIMULATOR

The point-target simulator, used in verifying the algorithm and making parameter selections, is shown in Fig. 2. The radar's parameters are specified in the left-top corner. Noise consists of thermal random noise, discrete sinusoidal tones, and narrow-band modulation signals (AM, FM, ...). They are characterized by their amplitudes, frequency locations, and bandwidths with respect to the radar signal. The option of using a sniffer pulse to periodically measure the RFI environment was incorporated. The combined radar-and-noise signal is fed into an A/D converter using either 8-bit or block-floating-point (BFPQ) quantization scheme. The A/D output is the input to the LMS adaptive filter which gives as its outputs the estimated RFI signal and the cleaned radar signal. In the examples shown in Fig. 3, the chirp signal has a bandwidth of 40 MHz and its signal-to-noise ratio (SNR) is 10 dB. The RFI consists of six tones and two FM signals. The tones are

at frequencies $\pm 3$, $\pm 10$, and $\pm 15$ MHz, with amplitudes (interference-to-signal ratio, ISR) 12, 13, and 17 dB, respectively. The FM signals have center frequencies of $\pm 12$ MHz, with bandwidths of 100 kHz (typical for FM radio channels), and ISRs of 15 dB. The initial phases of all RFI signals are picked at random.

## RESULTS

Fig. 3 shows the outputs of the pulse compression filter for the unfiltered, filtered, and ideal radar signals. The presence of RFI makes it difficult to detect the target (top graph). The adaptive filter helps in reducing the sidelobe energy and enhancing the target visibility (middle graph). The compressor output of the filtered signal compares favorably with the ideal case (bottom graph). Using the optimal design parameters obtained from the radar simulator, we have applied the TDLMS adaptive filter to a test site near Petaluma, California. The range-Doppler images of the scene is shown in Fig. 4. Compared with the RFI-contaminated images (top) the cleaned images (bottom) show remarkable improvement. The filter effectively removes artifacts (RFI stripes spread over the whole scene) and enhances the targets' visibility (such as streets and other small stand-alone features) which are difficult to detect from the top image.

## CONCLUSION

We have presented an adaptive filtering technique to remove RFI from wideband SAR signals. The filter employs the least-mean-square algorithm to update the filter weights. This weight update scheme requires no matrix solving or calculation of the correlation coefficients. The filter design is very simple since there are only three design parameters. Yet, the filter can adapt to the noisy RFI environment. We have also described the simulation procedure to show the filter's working principle and to obtain the optimal values for the design parameters. Finally, we have displayed the RFI-contaminated image and compared it with a much improved image. Our future efforts include fast versions of the adaptive filter and automatic determination of the design parameters.

**Acknowledgment:** The authors would like to thank Dr. M. Davis of DARPA and Dr. P. Tomlinson of DSA for their support and useful suggestions. This work has been done at the Jet Propulsion Laboratory, California Institute of Technology, under contract with the National Aeronautics and Space Administration.

# References

[1] M. Braunstein, J. Ralston, and D.Sparrow, "Signal processing approaches to radio frequency interference suppression", in *Algorithms for Synthetic Aperture Radar Imagery*, Dominick A. Giglio, Editor, *Proc. SPIE*, vol. 2230, pp.190-208, 1994.

[2] "Session 3: Radio Frequency Interference Rejection", in *Algorithms for Synthetic Aperture Radar Imagery II*, Dominick A. Giglio, Editor, *Proc. SPIE*, vol. 2487, pp. 72-129, 1995.

[3] B. Widrow, J. Glover, J. McCool, J. Kaunitz, C. Williams, K. Hearn, J. Zeidler, E. Dong, Jr., and R. Goodin, "Adaptive noise cancelling: principles and applications", *Proc. of the IEEE*, vol. 63, pp. 1692-1716, 1975.

[4] S. Haykin, *Adaptive Filter Theory*, Englewood Cliffs, N.J.: Prentice-Hall, 1991.

[5] Y. Kim, Y. Lou, J. van Zil, L. Maldonado, T. Miller, T. Sato, and W. Skotnicki, "NASA/JPL airborne three-frequency polarimetric/interferometric SAR system", in *Proc. IGARSS'96*, vol. 3, pp. 1612-14, Lincoln, NE, May 1996.

[6] P.A. Rosen, "IFSARE processor documentation", Jet Propulsion Laboratory, 1995.

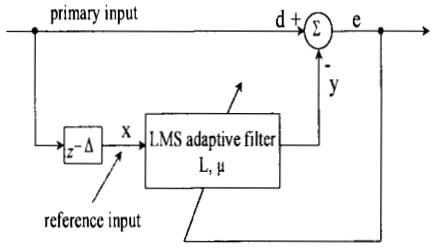


Figure 1: The LMS adaptive filter

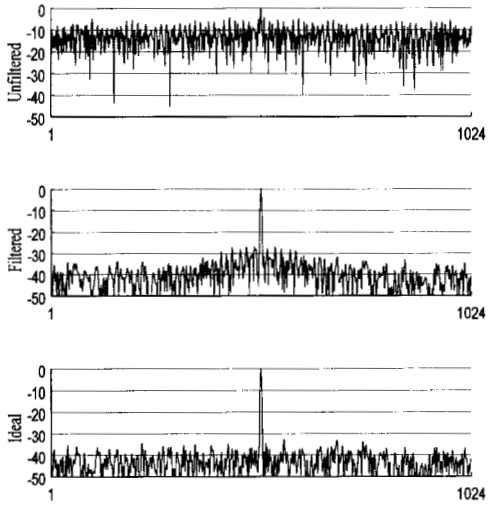


Figure 3: Comparison of outputs of pulse compression filter.

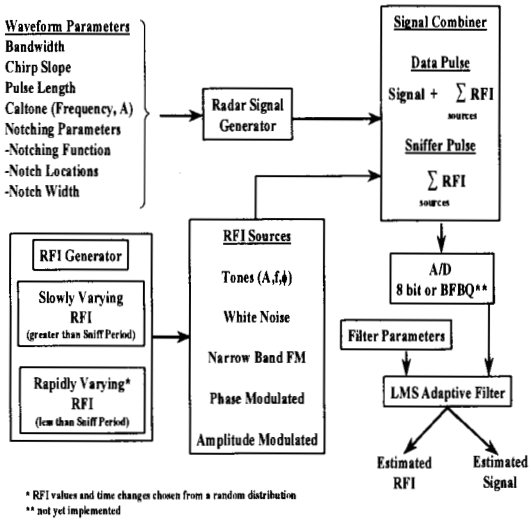


Figure 2: RFI Simulator Block Diagram

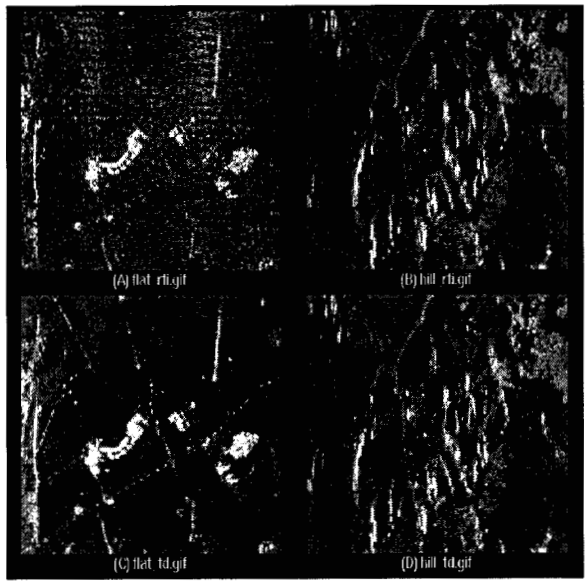


Figure 4: NASA/JPL P-band TOPSAR/AIRSAR images. (A) and (B) RFI contaminated rural and hilly areas, respectively; (C) and (D) same areas cleaned with LMS adaptive filter.